RSC Advances

ROYAL SOCIETY OF CHEMISTRY

www.rsc.org/advances

TOC

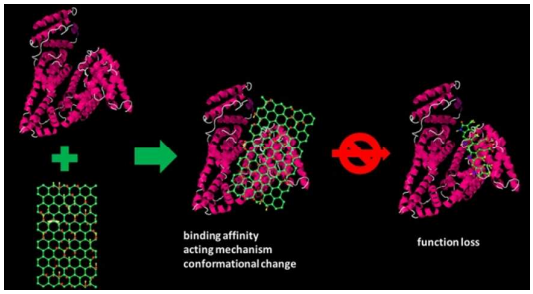

We show that GONS inhibits HSA function via two routes: blocking protein active sites, or destroying protein structure.

RSC Advances

RSCPublishing

COMMUNICATION

Interaction of Graphene Oxide with Human Serum Albumin and Its Mechanism

Cite this: DOI: 10.1039/x0xx00000x

Zhijia Ding,[a,b,c] Hongwei Ma [a] and Yanyan Chen [*,a]

Received ooth January 2012,
Accepted ooth January 2012

DOI: 10.1039/x0xx00000x

www.rsc.org/

Human serum albumin (HSA) is chosen to investigate the interaction of graphene oxide-based nanosheets (GONS) with plasma proteins in terms of binding affinity, action mechanism, conformational change and function loss. We show that GONS inhibit HSA function via two routes: blocking protein active sites, or destroying protein structure.

Graphene oxide (GO) with unique electrical, optical, chemical and mechanical properties[1] has found potential biotechnological applications in biosensor,[2-5] drug delivery system,[6-15] cellular imaging[6] and anti-cancer therapy[16-18]. Many biomedical applications of GO critically rely on its interaction with proteins.[19-22] Studies on the protein–GO interaction are essential for understanding GO's influence on structure and activities of proteins. Currently, such interaction studies have mainly focused on enzymes. Zhang et al[19,23] demonstrated that the biological activity of horseradish peroxidase (HRP) decreases after interaction with GO. Mrinmoy et al[24] reported that GO acts as an enzyme inhibitor to modulate the activity of α-Chymotrypsin but not induce conformational changes. However, for most in vivo biomedical applications of GO, GO will enter into the blood circulation system and inevitably makes contact with plasma proteins.[25] The interaction of plasma proteins with GO may interferer its blood circulation, cellular uptake and cause potential toxicity.[26] For example, the coating of plasma proteins on GO is proved to decrease its cytotoxicity.[27] But as reciprocity, it may induce an adverse effect on the adsorbent plasma proteins. To our knowledge, few reports referred to plasma protein interactions with GO exist. Only Zhang et al proved that GO induces conformation change and aggregation of HIV-1 regulatory protein.[28] Pattammattel et al mentioned that cationized BSA binds to GO with great affinity[29] without conformation or function study. GO is a two-dimensional nanomaterial with promising applications in biomedical field. Whether the GO-protein interaction induces structural or functional damage of plasma proteins and the mechanism of GO-protein interaction remain to be elucidated, which are of great importance to the normal function of blood.

Human serum albumin (HSA), the most abundant protein in plasma, plays crucial roles in binding and transporting a wide range of substances[30], including metal ions, fatty acids, amino acids, drug compounds, and metabolites such as bilirubin[31] and nitric oxide[32]. Therefore, we take HSA as an example to investigate the interaction between GO and human blood proteins in terms of binding affinity, action mechanism, conformational change and function loss. In addition, we also investigate the effect of surface properties of GO on HSA using 4 kinds of GO-based nanosheets (GONS, including GO, GO-COOH, GO-PEI and GO-CS), which are commonly used in drug delivery systems.

GO is prepared by Hummer's method[33] with minor modification and characterized with ultraviolet-visible spectroscopy, Fourier-transform infrared spectroscopy (FTIR), Raman spectroscopy, and atomic force microscopy (Figure S1). GO-COOH is obtained through oxidization of epoxy and hydroxyl groups on GO surface to carboxyl groups by chemical modification with sodium chloroacetate. GO-PEI or GO-CS is synthetized using carboxyl activating reagent (EDC) to initiate the formation of an amide linkage between GO and PEI (MW=25 KD) or CS (MW=10 KD), respectively. GONS are confirmed by FTIR (Figure S2) and a Zeta potential instrument (Figure S3). The schematic models of GONS are shown in Figure 1.

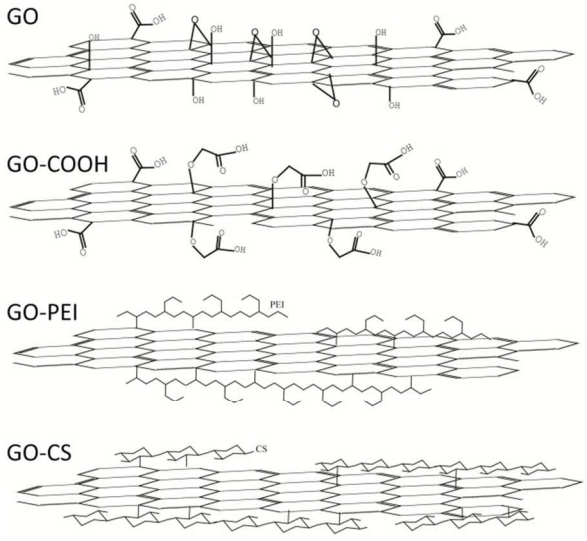

Figure 1 The schematic models of GONS.

Proteins are polymeric complexes of amino acids and contain fluorophores such as tyrosine, tryptophan, and phenylalanine, while GONS has the ability to significantly quench their intrinsic fluorescence by fluorescence resonance energy transfer (FRET).[34] Fluorescence quenching spectroscopy[35] is a convenient method for investigating the binding and conformational changes of proteins upon association with GONS. Based on fluorescence quenching intensity analysis, the binding and conformational changes of proteins upon association with GONS can be deduced. We first characterize the fluorescence quenches of HSA by GONS at different concentrations, as shown in Figure 2(a). It is evident that the increase in GONS concentration brings a progressive decrease in the emission maximum intensity of HSA.

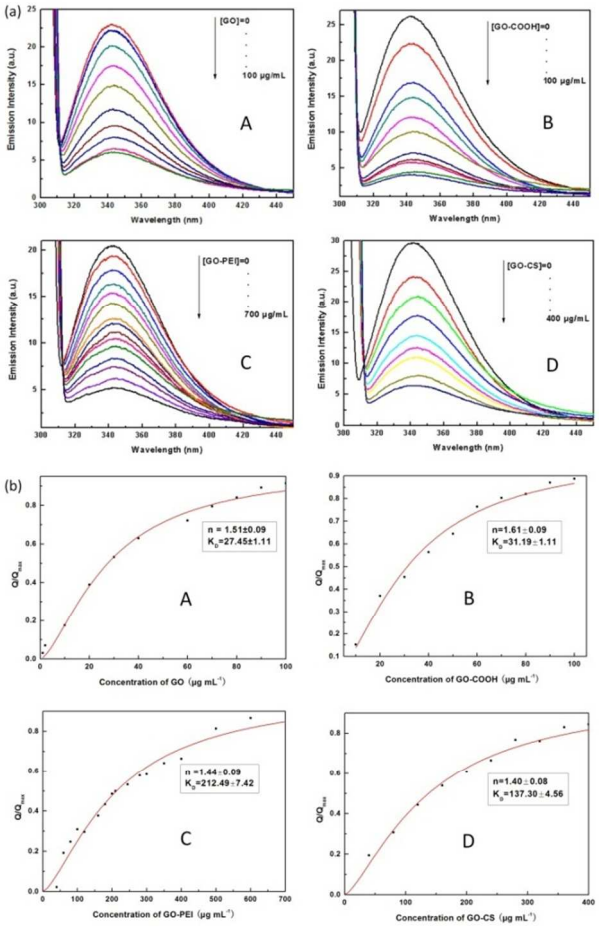

Figure 2 Fluorescence quenching measurements of HSA by GONS. (a) Fluorescence quenching spectra of HSA by GONS. (b) Binding constant calculated from fluorescence quenching measurements. (A) GO, concentration range is 0 to 100 μg mL^{-1}; (B) GO-COOH, concentration range is 0 to 100 μg mL^{-1}; (C) GO-PEI, concentration range is 0 to 700 μg mL^{-1}; (D) GO-CS, concentration range is 0 to 400 μg mL^{-1}.

In order to quantify the binding strength of HSA with GONS, the dissociation constant K_D is estimated based on the data in Figure 2(a). Considering the binding of HSA with GONS involves various driving factors including hydrogen bonds, electrostatic interactions, hydrophobic effects and π–π stacking effects etc,[36] HSA may have multiple binding sites with GONS. Therefore, we can expect the binding between HSA and GONS to exhibit cooperativity. Here the Hill equation (1) is used to deduce K_D by modelling Q through equation (2).[37]

$$\frac{Q}{Q_{max}} = \frac{[GO]^n}{K_D^n + [GO]^n} \quad (1)$$

$$Q = \frac{I^0 - I}{I^0} \quad (2)$$

where I_0 and I are fluorescence intensities in the absence and presence of GONS, respectively. Q_{max} is the saturation value of Q, K_D is the protein-GONS dissociation constant, and n is the Hill constant, which is generally regarded as a measure of association "cooperativity".

All K_D (Table 1) calculated from Hill equation as shown in Figure 2(b) are in the order of tens or hundreds μg mL^{-1}. This clearly shows GONS interact with HSA readily and the rank of the binding affinity of GONS to HSA is GO > GO-COOH > GO-CS > GO-PEI. The acting forces of HSA with GONS are complicated, may include covalent bonds, hydrophobic effects, hydrogen bonds, electrostatic interactions and π–π stacking effects etc. Isothermal titration calorimetry (ITC) provides a direct measurement of the thermodynamic parameters which allow attempts to be made to interpret the mechanism of binding through the direction of changes in enthalpy and entropy.[38] A favourable enthalpy change (negative ΔH) results from increased hydrogen bonding and often with subtle conformational changes. A favourable entropy change (positive ΔS) results from hydrophobic binding interactions. Therefore, the interaction of GONS with HSA is studied using ITC. Unlike the typical binding of two reacting species, the lack of accurate information of GONS (the molecular weights of GONS are nonuniform and unknown) precludes plotting the binding isotherms against a molar ratio. Consequently, we plot the binding isotherms against the total volume of HSA added to the reaction cell and will merely identify the direction of enthalpy changes and entropy changes.[39] From the results of ITC shown in Figure 3, negative ΔH are found in the interaction of HSA with GO or GO-COOH, which means hydrogen bonds are main acting forces. ITC only provides useful information about non-covalent interactions. As we all know, GO consists of oxygen functional groups such as hydroxyl, carboxy1 and epoxy groups.[40] The epoxy groups can react with amine through nucleophilic addition reaction[41-43] under mild conditions. Without a doubt, covalent bonds are formed during the interaction of GO with HSA between epoxy groups on GO and the Lys and Arg on the surface of HSA. So, we can expect that the main driving forces of GO binding HSA are covalent bonds and hydrogen bonds. The binding of GO-COOH to HSA are mainly governed by hydrogen bonds because the epoxy groups are blocked by carboxyl groups. For the interaction of GO-PEI or GO-CS with HSA, from the unfavourable enthalpy changes and negative ΔG (Gibbs free energy change, a spontaneous binding reaction suggests negative ΔG), we can deduce the positive ΔS using the relation in Equation 3,

$$\Delta G = \Delta H - T\Delta S \quad (3)$$

Positive ΔS indicate that hydrophobic forces contribute to the interaction of GO-PEI or GO-CS with HSA. The turning points in Figure 3C, D may indicate another binding mechanism forms after initial hydrophobic interactions, which could induce structural changes of HSA upon the exposure of its inner structure to GONS.

Table 1 Comparison of the interaction of different GONS with HSA.

	K_D (μg mL^{-1})	λ_{max} (nm)	α-helix (%)	*BBC* (%)
Control	/	342.4±0.4	61.5±0.6	100
GO	27.5±1.1	343.8±0.6	48.6±0.6	34.7±6.1
GO-COOH	31.2±1. 1	343.2±0.3	55.7±0.9	96.3±8.2
GO-PEI	212.5±7.4	345.2±0.6	23.8±2.9	4.9±0.6
GO-CS	137.3±4.6	344.0±0.4	53.5±1.8	77.9±4.7

All the values above are the mean of three replicate measurements.

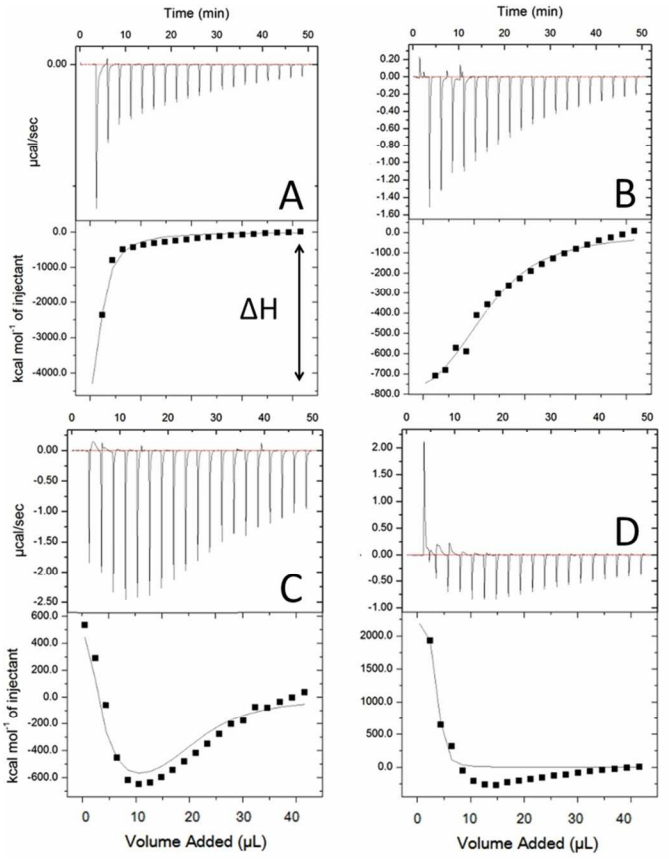

Figure 3 ITC titration data describing the interaction of HSA with GONS. (A) GO; (B) GO-COOH; (C) GO-PEI; (D) GO-CS. The upper part of each figure shows the raw calorimetric data obtained during injection of 3×10^{-5} M HSA into the calorimetric cell containing 100 μg mL^{-1} GONS. The lower half shows the integrated data of the curves respectively plotted as a function of total volume of HSA solution added to the reaction cell, after removed the heat change in dilution processes.

The results of zeta potential (Figure S3) indicate that GONS are nanosheets with strong charges. To elucidate whether electrostatic interactions contribute to the interaction between GONS and HSA, the binding of GONS with HSA is studied in PBS with pH from 4.0 to 9.0 through fluorescence quenching measurements. The results are shown in Figure 4 where lower fluorescence intensity suggests a stronger interaction. For GO, we find the interaction of GO with HSA is stronger with the decrease of pH. GO is negatively charged when pH varies from 4.0 to 9.0 (zeta potentials of GONS in PBS with different pH are shown in Table S1). HSA's isoelectric point is about 4.7. Thus, positively charged HSA interacts with negatively charged GO by electrostatic interactions at the condition of pH 4.0. While in PBS from pH 5.5 to 9.0, both HSA and GO are negatively charged. We all know like charges repel each other. However, the electrostatic interactions cannot be thoroughly excluded because protein is net charged and there are still positively charged regions on protein surface. Similar results are found between GO-COOH and HSA. GO-CS is positively charged in PBS with pH from 4.0 to 9.0. When pH varies from 5.5 to 9.0, negatively charged HSA is supposed to interact with positively charged GO-CS by electrostatic interactions. At pH 4.0, GO-CS and HSA have like positive charges so that the electrostatic interactions are weakened. But GO-CS still shows a stronger binding with HSA. The probable reason is that hydrophobic bindings contribute to the interaction between GO-CS and HSA since HSA show the strongest hydrophobicity at the environment near isoelectric point. For GO-PEI, it is positively charged when pH varies from 4.0 to 9.0. HSA shows more net negative charge with the increase of pH. Consequently, the gradually stronger binding between GO-PEI and HSA shown in Figure 4 proves that electrostatic interactions play an important role in their interaction. Based on the results of ITC and pH dependence study, we can conclude that the dominate forces of the binding of GO with HSA are covalent bonds as well as hydrogen bonds, and GO-COOH interacts with HSA mainly via hydrogen bonds. The electrostatic interactions cannot be excluded for these two negatively charged GONS. For positive charged GO-PEI and GO-CS, both electrostatic and hydrophobic interactions contribute to their interactions with HSA. Besides, because of the sp^2 carbon structure in graphenes, π–π stacking is one of the main driving forces for interactions between proteins and graphenes.[36,44] GONS are derivations of graphene and sp^2 carbon structure is also involved in GONS, which means π–π stacking cannot be ignored.

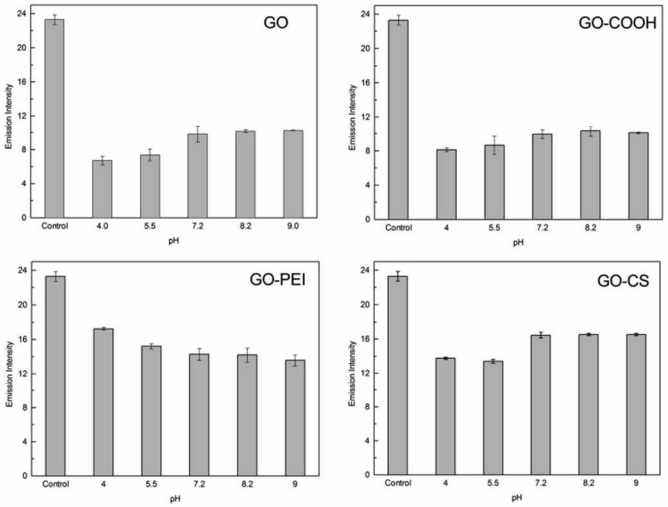

Figure 4 pH influence on the interaction between GONS and HSA.

The Hill constant *n*, a frequently utilized measure of binding cooperativity, is calculated in Figure 2(b). We notice that all *n* are >1, which indicates that GONS-HSA interaction is a positively cooperative reaction, meaning that once one GONS molecule binds to HSA, its affinity for HSA progressively increases. The probable reason is that HSA have multiple binding sites with GONS and a part of them are buried inside the protein structure. Once one GONS binds, the interaction induces protein conformational changes (the results are proved in the next part), then protein will expose the inner binding sites to make GONS show progressively increasing binding affinity for HSA.

In order to verify this possibility of protein conformational changes while HSA interacted with GONS, we perform the following work. HSA contains only one tryptophan residue (Trp-214),[45] which is an important fluorescent probe that is extremely sensitive to the nature of the microenvironment of Trp-214.[46] In other words, microenvironment changes of Trp-214 are related to the conformational changes of HSA and can be evaluated by measuring changes in the peak intensity wavelength (λ_{max}) in the fluorescence emission spectrum. To our study, λ_{max} has a red shift when HSA interacts with GONS, as shown in Figure 5(a). The red shift of λ_{max} means that Trp-214 is exposed in a more hydrophilic environment [46] as a result of conformational changes.

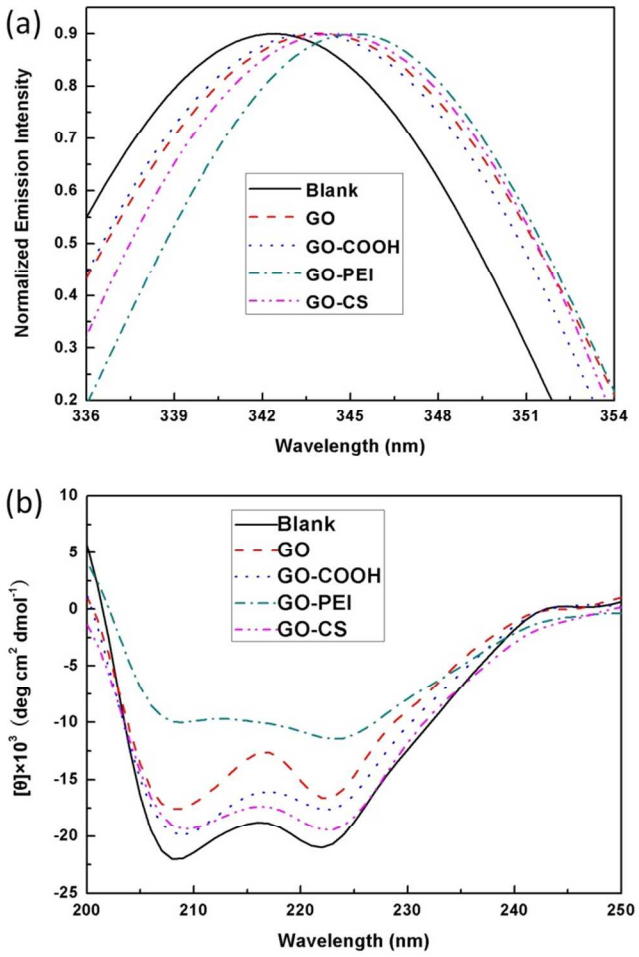

Figure 5 Effect of GONS on the structure of HSA. (a) The red shift of λ_{max} induced by the interaction of GONS with HSA. (b) Effect of GONS on HSA secondary structure determined by CD spectra.

The circular dichroism (CD) spectrum in the far UV region (180 nm-250 nm) can probe the secondary structure of proteins.[35,37,47,48] It is a powerful tool to quantify the conformational changes of HSA after absorbed onto GONS. HSA structure is predominantly α-helical (approximately 67%) and its CD spectrum reveals two negative bands in the ultraviolet region at 208 and 222 nm.[37,48] The MRE values at 208 nm reflect the α-helix content of HSA. After 2 hour incubation with GONS, the CD spectra of HSA in the presence of GONS are shown in Figure 5(b). The α-helix content is calculated based on equations (4) and (5).[47]

$$\propto -helix(\%) = \frac{[-MRE_{208} - 4000]}{[33000 - 4000]} \times 100 \quad (4)$$

$$\mathrm{MRE}_{208} = \frac{\theta \cdot M}{10 \cdot C \cdot L \cdot N_r} \quad (5)$$

where θ is the ellipticity value of the sample, M is the molecular weight (Da) of HSA, C is the HSA concentration (mg mL^{-1}), L is the sample cell path length (cm), and N_r is the number of amino residues.

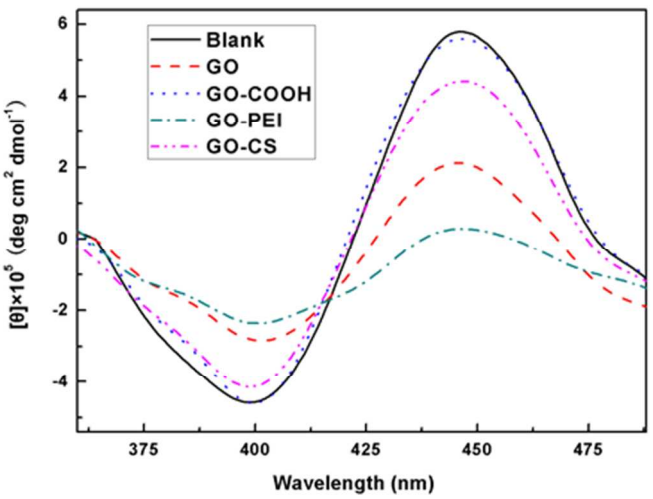

Figure 6 Effect of GONS on HSA function determined by cotton effect of the bilirubin binding to GONS-associated HSA.

Table 1 shows no significant decline of the α-helix content of HSA after association with 4 types of GONS except GO-PEI, and the rank of the adverse effect of GONS on HSA conformational is GO-PEI > GO > GO-CS > GO-COOH. Obviously, GO-PEI causes the greatest damage to the structure of HSA due to strong electrostatic and hydrophobic interactions. GO-CS also binds with HSA via these two driving forces, but it leads to mild structure changes since it has a lower quantity of positive charge than GO-PEI. The major forces of the GO-HSA interaction are hydrogen bonds and covalent bonds. All these forces are on the surface and make HSA be in relatively close proximity to the native state. But the abundant epoxy groups on GO covalently bind to the surface amino residues of HSA, generating a lot of crosslinks. The presence of these crosslinks in partially unfolded state will result in a more compact unfolded state[49,50] which means some changes of HSA structure. GO-COOH is obtained through the modification of epoxy groups with polar carboxyl groups and the epoxy groups are therefore blocked. So no crosslinks form in the interaction of GO-COOH with HSA, which leads to subtle conformational changes.

It is widely acknowledged that proteins being in non-native conformations are devoid of normal biological function. The results in Figure 5 quantify the conformational changes of HSA after absorbed onto GONS. We are wondering whether GONS's binding onto proteins affect the native functions of the proteins. HSA works in binding and delivering bilirubin, a toxic metabolite of heme. Fortunately, a cotton effect curve is observed in the visible region by CD measurement for bilirubin-HSA complex and the amplitude is in proportion to the complex amount.[32] In our experiment, the cotton effect curves of bilirubin binding to different GONS-associated HSA are measured by CD to verify HSA functional changes in bilirubin binding and the results are shown in Figure 6. The bilirubin binding capacity (*BBC*) of HSA associated with GONS is calculated by equation (6) to better understand the functional change of HSA influenced by GONS.

$$BBC(\%) = \frac{\theta_{peak,GONS}}{\theta_{peak}} \times 100 \quad (6)$$

where θ_{peak} is the peak ellipticity value of bilirubin-native HSA complex and $\theta_{peak,GONS}$ is that of bilirubin-GONS associated HSA complex.

The results demonstrate that the *BBC* of HSA is clearly reduced after association with GONS except GO-COOH (Table 1), and the rank of the adverse effect of GONS on HSA function is GO-PEI > GO > GO-CS > GO-COOH (The influence of GONS competitive

binding bilirubin is discussed in Figure S4 and it is negligible). The tendency of the effect of GONS on HSA functional changes is in accordance with that on HSA conformation. This means the conformational change of HSA is an important factor to its functional change. On the other hand, GO does not cause serious conformational change of HSA, but its *BBC* only maintains at 34.7±6.1. It is probably due to the crosslinks in GO-HSA. The covalent bonds between GO and HSA are nonspecific and the binding sites of HSA to GO may be around the bilirubin binding site, making the HSA active site blocked and leading to the malfunction of bilirubin binding.

Conclusions

This study demonstrates that GONS readily interact with HSA, making GONS appropriate for protein-GONS complex assembly. The driving forces of the binding include covalent bonds, hydrogen bonds, electrostatic forces, hydrophobic interactions and π–π stacking effects etc. However, pristine GO may induce conformational changes in HSA and malfunction in HSA's binding capacity to toxins, leading to potential toxicity. We can conclude that GO is a potential substance to easily immobilize protein though it inhibit the protein's function. It consists with the result of Zhang et al[23] that the enzyme immobilization on the GO sheets can take place readily without using any cross-linking reagents, though the enzyme activity decreases. After surface modification, GO-COOH interacts with HSA mainly through hydrogen bonds. It shows best biocompatibility to HSA with minimum conformational and functional changes. This indicates that GO-COOH is an optimal substance for protein self-assembly and also a promising graphene nanomaterial for biomedical applications. GO-CS exhibits similar but slightly worse biocompatibility to HSA than GO-COOH, while GO-PEI almost destroys the structure and function of HSA. Also, we have found two potential routes for GONS influence on HSA's function. GO inhibits the function of HSA mainly through blocking the protein active site, and GO-PEI affects the function of HSA through the disruption of protein structure.

In this paper, HSA is taken as an example to investigate the effect of GONS on blood proteins. However, since blood components are complicated, comprehensive studies of GONS with blood proteins would help to understand the fate of GONS in living bodies. Further work on this topic is warranted.

Notes and references

[a] Key Laboratory for Nano-Bio Interface Research, Division of Nanobiomedicine, Suzhou Institute of Nano-Tech and Nano-Bionics, Chinese Academy of Sciences, Suzhou, 215123, P.R. China. E-mail: Yanyanchen2006@sinano.ac.cn

[b] Institute of Biophysics, Chinese Academy of Sciences, Beijing, 100101, P.R. China

[c] University of Chinese Academy of Sciences, Beijing, 100039, P.R. China

Electronic Supplementary Information (ESI) available: [details of any supplementary information available should be included here]. See DOI: 10.1039/c000000x/

1 Geim, A. K. *Science* **2009**, *324*, 1530.

2 Wang, Y.; Li, Z.; Hu, D.; Lin, C. T.; Li, J.; Lin, Y. *J. Am. Chem. Soc.* **2010**, *132*, 9274.

3 Kuila, T.; Bose, S.; Khanra, P.; Mishra, A. K.; Kim, N. H.; Lee, J. H. *Biosens. Bioelectron.* **2011**, *26*, 4637.

4 Wang, Y.; Li, Z. H.; Wang, J.; Li, J. H.; Lin, Y. H. *Trends Biotechnol.* **2011**, *29*, 205.

5 Shao, Y.; Wang, J.; Wu, H.; Liu, J.; Aksay, I. A.; Lin, Y. *Electroanal.* **2010**, *22*, 1027.

6 Sun, X. M.; Liu, Z.; Welsher, K.; Robinson, J. T.; Goodwin, A.; Zaric, S.; Dai, H. J. *Nano Res.* **2008**, *1*, 203.

7 Yang, X. Y.; Zhang, X. Y.; Liu, Z. F.; Ma, Y. F.; Huang, Y.; Chen, Y. *J. Phys. Chem. C* **2008**, *112*, 17554.

8 Zhang, L. M.; Lu, Z. X.; Zhao, Q. H.; Huang, J.; Shen, H.; Zhang, Z. J. *Small* **2011**, *7*, 460.

9 Feng, L. Z.; Zhang, S. A.; Liu, Z. A. *Nanoscale* **2011**, *3*, 1252.

10 Dong, H. F.; Ding, L.; Yan, F.; Ji, H. X.; Ju, H. X. *Biomaterials* **2011**, *32*, 3875.

11 Liu, Z.; Robinson, J. T.; Sun, X. M.; Dai, H. J. *J. Am. Chem. Soc.* **2008**, *130*, 10876.

12 Yang, X. M.; Tu, Y. F.; Li, L. A.; Shang, S. M.; Tao, X. M. *ACS Appl. Mater. Inter.* **2010**, *2*, 1707.

13 Ha, C. S.; Rana, V. K.; Choi, M. C.; Kong, J. Y.; Kim, G. Y.; Kim, M. J.; Kim, S. H.; Mishra, S.; Singh, R. P. *Macromol. Mater. Eng.* **2011**, *296*, 131.

14 Bao, H. Q.; Pan, Y. Z.; Ping, Y.; Sahoo, N. G.; Wu, T. F.; Li, J.; Gan, L. H.; Li, L. *Small* **2011**, *7*, 1569.

15 Zhang, L. M.; Xia, J. G.; Zhao, Q. H.; Liu, L. W.; Zhang, Z. J. *Small* **2010**, *6*, 537.

16 Tian, B.; Wang, C.; Zhang, S.; Feng, L.; Liu, Z. *ACS Nano* **2011**, *5*, 7000.

17 Robinson, J. T.; Tabakman, S. M.; Liang, Y.; Wang, H.; Sanchez Casalongue, H.; Vinh, D.; Dai, H. *J. Am. Chem. Soc.* **2011**, *133*, 6825.

18 Yang, K.; Zhang, S. A.; Zhang, G. X.; Sun, X. M.; Lee, S. T.; Liu, Z. A. *Nano Lett.* **2010**, *10*, 3318.

19 Zhang, Y.; Zhang, J. Y.; Huang, X. L.; Zhou, X. J.; Wu, H. X.; Guo, S. W. *Small* **2012**, *8*, 154.

20 Liu, P.; Zhang, X.; Feng, L.; Xiong, H.; Wang, S. *Am. J. Biomed. Sci.* **2011**, *3*, 69.

21 Kang, X.; Wang, J.; Wu, H.; Aksay, I. A.; Liu, J.; Lin, Y. *Biosens. Bioelectron.* **2009**, *25*, 901.

22 Jung, J. H.; Cheon, D. S.; Liu, F.; Lee, K. B.; Seo, T. S. *Angew. Chem. Int. Ed.* **2010**, *49*, 5708.

23 Zhang, J.; Zhang, F.; Yang, H.; Huang, X.; Liu, H.; Zhang, J.; Guo, S. *Langmuir* **2010**, *26*, 6083.

24 De, M.; Chou, S. S.; Dravid, V. P. *J. Am. Chem. Soc.* **2011**, *133*, 17524.

25 Patravale, V. B.; Date, A. A.; Kulkarni, R. M. *J. Pharm. Pharmacol.* **2004**, *56*, 827.

26 Dobrovolskaia, M. A.; Aggarwal, P.; Hall, J. B.; McLeland, C. B.; McNeil, S. E. *Adv. Drug Deliver. Rev.* **2009**, *61*, 428.

27 Hu, W. B.; Peng, C.; Lv, M.; Li, X. M.; Zhang, Y. J.; Chen, N.; Fan, C. H.; Huang, Q. *ACS Nano* **2011**, *5*, 3693.

28 Zhang, M.; Mao, X. B.; Wang, C. X.; Zeng, W. F.; Zhang, C. L.; Li, Z. J.; Fang, Y.; Yang, Y. L.; Liang, W.; Wang, C. *Biomaterials* **2013**, *34*, 1383.

29 Pattammattel, A.; Puglia, M.; Chakraborty, S.; Deshapriya, I. K.; Dutta, P. K.; Kumar, C. V. *Langmuir* **2013**, *29*, 15643.

30 Fehske, K. J.; Muller, W. E.; Wollert, U. *Biochem. Pharmacol.* **1981**, *30*, 687.

31 Simon, D. I.; Stamler, J. S.; Jaraki, O.; Keaney, J. F.; Osborne, J. A.; Francis, S. A.; Singel, D. J.; Loscalzo, J. *Arterioscler. Thromb.* **1993**, *13*, 791.
32 Blauer, G.; Harmatz, D.; Naparste.A *Febs. Lett.* **1970**, *9*, 53.
33 Hummers, W. S.; Offeman, R. E. *J. Am. Chem. Soc.* **1958**, *80*, 1339.
34 Lu, C. H.; Yang, H. H.; Zhu, C. L.; Chen, X.; Chen, G. N. *Angew. Chem. Int. Ed.* **2009**, *121*, 4879.
35 Chen, Y. L.; Zhang, X. F.; Gong, Y. D.; Zhao, N. M.; Zeng, T. Y.; Song, X. Q. *J. Colloid. Interf. Sci.* **1999**, *214*, 38.
36 Mu, Q.; Jiang, G.; Chen, L.; Zhou, H.; Fourches, D.; Tropsha, A.; Yan, B. *Chem. Rev.* **2014**, *114*, 7740.
37 Lacerda, S. H. D.; Park, J. J.; Meuse, C.; Pristinski, D.; Becker, M. L.; Karim, A.; Douglas, J. F. *ACS Nano* **2010**, *4*, 365.
38 Holdgate, G. A. *Expert Opinion on Drug Discovery* **2007**.
39 Joshi, H.; Shirude, P. S.; Bansal, V.; Ganesh, K.; Sastry, M. *The J. Phys. Chem. B* **2004**, *108*, 11535.
40 Lerf, A.; He, H. Y.; Forster, M.; Klinowski, J. *J. Phys. Chem. B* **1998**, *102*, 4477.
41 Azizi, N.; Saidi, M. R. *Org. Lett.* **2005**, *7*, 3649.
42 Chattopadhyay, S.; Keul, H.; Moeller, M. *Macromol. Chem. Phys.* **2012**, *213*, 500.
43 Ziyaei-Halimehjani, A.; Gholami, H.; Saidi, M. R. *J. Iran. Chem. Soc.* **2013**, *10*, 7.
44 Liang, L. J.; Wang, Q.; Wu, T.; Shen, J. W.; Kang, Y. *Chin. J. Chem. Phys.* **2009**, *22*, 627.
45 Meloun, B.; Moravek, L.; Kostka, V. *Febs. Lett.* **1975**, *58*, 134.
46 Lim, B. T.; Kimura, T. *J. Biol. Chem.* **1980**, *255*, 2440.
47 Greenfield, N.; Fasman, G. D. *Biochemistry* **1969**, *8*, 4108.
48 Li, L. W.; Mu, Q. X.; Zhang, B.; Yan, B. *Analyst* **2010**, *135*, 1519.
49 Myers, J. K.; Nick Pace, C.; Martin Scholtz, J. *Protein Science* **1995**, *4*, 2138.
50 Barthelmebs, L.; Carpentier, R.; Rouillon, R. In *Photosynthesis Research Protocols*; Springer: **2011**, 247.

